Materials Science and Engineering C 68 (2016) 338–342

Contents lists available at ScienceDirect

Materials Science and Engineering C

journal homepage: www.elsevier.com/locate/msec

Immunosensor for diagnosis of Alzheimer disease using amyloid-β 1–40 peptide and silk fibroin thin films

J.M. Gonçalves [a], L.R. Lima [a], M.L. Moraes [b,*], S.J.L. Ribeiro [a]

[a] Instituto de Química, Universidade Estadual Paulista "Júlio de Mesquita Filho" UNESP, Rua Professor Francisco Degni, 55, 14800-060 Araraquara, SP, Brazil
[b] Instituto de Ciência e Tecnologia, Universidade Federal de São Paulo UNIFESP, Rua Talim, 330, 12231-280 São José dos Campos, SP, Brazil

ARTICLE INFO

Article history:
Received 7 March 2016
Received in revised form 13 May 2016
Accepted 23 May 2016
Available online 24 May 2016

Keywords:
Alzheimer's disease
Immunosensor
Silk fibroin
Layer-by-layer
Amyloid-β peptide

ABSTRACT

Layer-by-Layer (LbL) films containing silk fibroin (SF) and the 40 aminoacid-long amyloid-β peptide (Aβ1-40) were prepared with the purpose of developing a new prototype of an electrochemical immunosensor. The film showed a satisfactory growth in quartz substrate and screen-printed carbon electrodes, as observed by UV–vis spectroscopy and cyclic voltammetric, respectively. The peptide immobilized in LbL films in junction with SF shows secondary structure induced, as shown by circular dichroism measurements, favoring the interaction SF/peptide LbL film with the specific antibody. Immunosensor showed a linear response in the presence of the antibody with concentrations from 0 to 10 ng mL^{-1} both analyzed by current changes in 0.3 V and voltammogram area. This system can be applied as a new prototype for preliminary diagnosis of Alzheimer's disease.

1. Introduction

Alzheimer's disease (AD) is the most common type of progressive senile dementia affecting specially the elderly over 65 years of age, although some cases exist for younger people [1]. It is estimated that until 2050 there will be 106.23 million AD cases worldwide [2], and the economic burden for treatment, including special care that patients need, is approximately 604 billion dollars [3]. The cause of AD is not well understood and the diagnosis is only reliable on biomarkers if cognitive decline is already pronounced [4].

The disease is characterized by formation of neurofibrillar tangles and aggregation of amyloid β (Aβ) in extracellular plaques in the affected regions of the brain [5]. Thus, clinical diagnoses could possibly be performed using imaging, such as computed tomography [6] or magnetic resonance imaging [7], and/or cerebral spinal fluid or blood tests [4,8]. There are some biomarkers that can be used in blood tests, including platelet amyloid precursor protein, levels of amyloid β (Aβ) or autoantibodies against Aβ in the plasma or serum [9]. Platelet are mainly consisted of the 40 amino acid-long Amyloid β (Aβ1–40) [4], thus drawing much attention as a biomarker for AD. It is believed that conformational changes of Aβ1–40 from random coil to β-sheet when bound to membranes are responsible for the formation of membrane pores, inducing ion permeability especially of calcium that can trigger cell death or apoptosis signaling [5].

Superparamagnetic iron oxide nanoparticles (SPIONs) were investigated as a brain Aβ1-40 fibril imaging, that showed a great increase in its fluorescence signal, which could lead to the successful imaging of these fibrils [10]. In fact, SPIONs recently also showed to affect the Aβ fibrillation process, thus providing a possible theragnostics platform [11].

Excluding imaging diagnosis, there are other several approaches for biosensors using Aβ1–40, including infrared spectroscopy [12] that was effective to detect a concentration of 50 $\mu g \cdot mL^{-1}$ in deuterated water solution and cyclic voltammetry using an electrode modified with antibodies that obtained a linear response from 400 $nmol \cdot L^{-1}$ to 2000 $nmol \cdot L^{-1}$ [13]. Both of them would probably result in a long preparation time or elevated price for large-scale applications.

More recently an electrochemical method for Aβ1–40 detection using cyclic voltammetry was described [14]. A gold electrode was modified with a peptide that promoted fibrillation of Aβ1-40, which resulted in a difference in the anodic peak of the cyclic voltammograms. The anodic peak was proportional to the Aβ1-40 concentration. The disadvantage of this method is the need for electrode modification. A colorimetric detection of Aβ1-40 was also described recently. In the presence of Cu^{2+} ions, the peptide could interact with gold nanoparticles, promoting its aggregation and, therefore, a shift in its absorbance from red to blue, giving a linear response from 0 to 300 $nmol.L^{-1}$ of concentration [15].

A new immunosensor for *anti*-Aβ1-40 antibodies detection is proposed here. The strategy includes the combination of silk fibroin (SF) that is a versatile material, for immobilization of the amyloid β peptide (Aβ1-40). Self-assembly films were prepared by the Layer-by-Layer (LbL) technique. Detection method used was a simple monitoring of

* Corresponding author.
E-mail address: marli.moraes@gmail.com (M.L. Moraes).

http://dx.doi.org/10.1016/j.msec.2016.05.101
0928-4931/

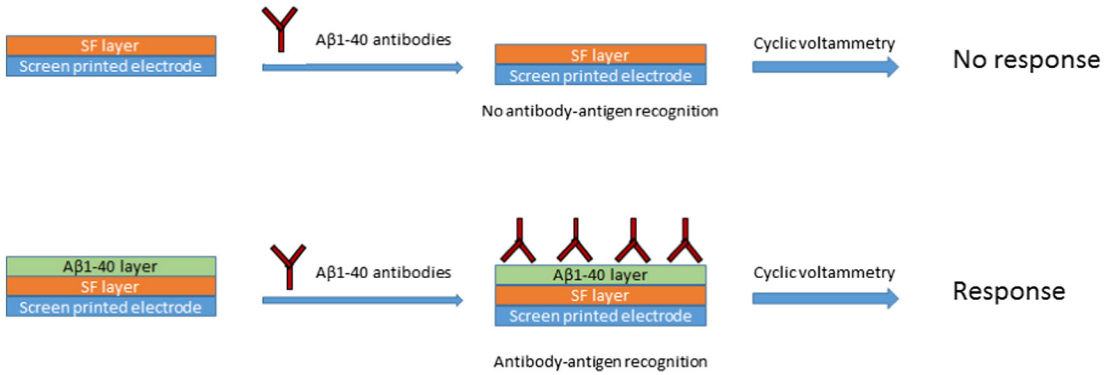

Fig. 1. Scheme of antibody recognition on screen-printed carbon electrodes with 1-layer and 1-bilayer SF/Aβ1-40.

the specific antibody adsorption over the film by cyclic voltammetry measurements.

Layer-by-layer (LbL) films [16] are multilayer films of polyions of opposite charges adsorbed alternating the adsorption. Although charges are important for LbL film assembly, it is known that LbL films can also be prepared by the action of other interactions, such as hydrogen bonding [17]. This gives more versatility for the components of films. In fact, several applications of LbL films are described in literature, including enzyme biosensors and immunosensors [18].

Silk fibroin (SF) is a biocompatible material extracted from natural silk and exhibits excellent mechanical and structural properties [19, 20]. *Bombyx mori* silk fibroin consists of a light chain protein and a heavy chain protein bonded together by a disulfide bond [21]. Its LbL films were already studied and showed consistent growth up to 12 layers [22]. In addition to the fact that SF can be auto adsorbed in LbL films, it is believed that it can induce secondary structure in peptides for immunosensing applications [23].

2. Materials and methods

2.1. Materials

Synthetic Aβ1-40 peptide (DAEFRHDSGYEVHHQKLVFFAEDVGSNKGAI IGLMVGGVV) was purchased from PhtdPeptides Co. (Zhengzhou, China) with 90% purity (Molecular weight: 4239.8 g mol^{-1}; theoretical pI 5.31). *Anti*-Aβ1–40 monoclonal antibodies type IgG were purchased from Santa Cruz Biotechnology Inc. (Dallas, U.S.A.) with 200 μg mL^{-1} concentration.

The *Bombyx mori* cocoons, produced by the larvae of *Bombyx mori*, used in this work were acquired from BRATAC SA. (Brazil). The cocoon consists of hull, and spoil chrysalis, wherein the shell consists mainly of sericin and fibroin. These cocoons have a pearly white color and oval shape.

Screen-printed carbon electrodes were purchased from DropSens (Oviedo, Spain), with a 4 mm diameter working electrode, Ag reference electrode and carbon counter electrode. All other reagents were purchased from Synth.

2.2. Solutions

Silk fibroin was extracted from the cocoons of the *Bombyx mori* silkworm. Initially, cocoons were cut and boiled in Na_2CO_3 0.02 mol L^{-1} during 30 min to removed sericin. The silk fibers obtained were dissolved in $CaCl_2$:Ethanol:Water (1:2:8 mol) at 60 °C and dialyzed in MilliQ water at room temperature for 48 h. The SF concentration was approximately 3% (m/m).

Stock solution 10 mg mL^{-1} Aβ1–40 in DMSO was prepared to prevent peptide aggregation. [12] The solution utilized for the preparation of the films was diluted to 0.5 mg mL^{-1} in purified MilliQ water.

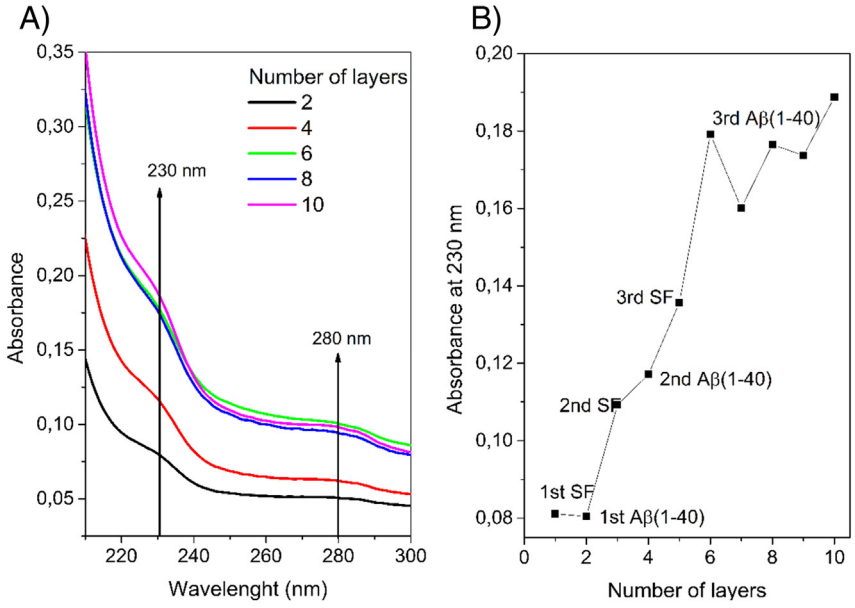

Fig. 2. (A) Absorption spectra of the SF + Aβ1-40 film at each layer adsorbed in quartz substrate. (B) Absorption in 230 nm as a function of the number of layers.

The *anti*-Aβ1-40 antibodies were diluted in phosphate buffer solution (PBS) pH 7.4 to the required concentration.

2.3. Film preparation and characterization

The film was grown in quartz substrate which was submitted in SF 0.1% m/m solution for 10 min. After adsorption of SF the film was washed in purified MilliQ H_2O and dried in N_2 flux. The same was done in Aβ1-40 0.5 mg·mL^{-1} solution.This procedure was repeated until the adsorption of the number of layers required. In the case of carbon electrodes, the same procedure was performed, but instead of submerging the electrode in the solutions, a small amount of the solutions was deposited in the working electrode.

The film characterization and its growth were conducted by UV–vis spectroscopy and cyclic voltammetry. These measurements were performed in triplicate.

Circular dichroism measurements were conducted to investigate the secondary structure of the proteins in the film.

UV–vis spectroscopy was performed in a Varian Inc. Cary® 50 spectrophotometer, with 1 nm slits; cyclic voltammetry was performed in DropSens μStat with 50 mV s^{-1} scan rate and circular dichroism in a Jasco Inc. J-815 spectrometer with band width 5 nm, data pitch 0.2 nm and scan rate 50 nm min^{-1}.

2.4. Detection

Detection of the *anti*-Aβ1–40 antibody was conducted by adding 200 μL of each solution with certain concentration in the electrode for 10 min followed by washing with PBS buffer to eliminate any antibody residue not adsorbed. To perform measurements 400 μL of PBS buffer was added to the electrode and the cyclic voltammogram was obtained. The films used for detection have been prepared with 1 SF layer or 1 SF/Aβ1-40 bilayer, as shown in Fig. 1.

3. Results and discussion

The peptide immobilization in quartz substrate was investigated by UV–Vis spectroscopy. It is known that SF can adsorb over itself in LbL films [22] and it was used for immobilize specific peptides [23], but the adsorption of the Aβ1–40 peptide over SF has not described in the literature.

The LbL film containing SF and Aβ1-40 showed an absorption band in 230 nm that can be attributed to the peptide bond and a discreet band positioned at 280 nm, possibly attributed to tyrosine amino acid present in the peptide sequence, as shown in Fig. 2A. The peptide bond band increased gradually from 0.08 to 0.19 when more layers were grown. The gradual increase was evidence when SF and Aβ1-40 were being added to the quartz substrate. The adsorption of peptide over SF can be explained by weak intermolecular interactions (for example the hydrogen bonding) between SF and Aβ1-40. Since the theoretical isoelectric point of SF is 4.39 [24] and of Aβ1-40 is 5.31 and as both are at pH ≈ 6 they are with a slightly negative charge.

Fig. 2B shows absorbance at 230 nm for each layer deposited. It is noted that absorbance of the first SF layer to first Aβ1-40 layer showed no significant change. This effect can be attributed to the quartz surface defects. After 1-bilayer SF/Aβ1-40 until 3-bilayers SF/Aβ1-40 the absorbance increases almost linearly for each layer deposited, confirming that both SF as peptide were being gradually adsorbed to the quartz substrate. This almost linear increase can be attributed to deposition time or defects on the surface of the quartz substrate. From the third bilayer the LbL film growth showed irregular. Thus, for detection measurements LbL films were assembled containing 1, 3 and 5 bilayers.

Concerning the immunosensor device, the detection was performed by using screen printed carbon electrodes. In this case the film growth was also investigated on the electrode surface using cyclic voltammetry, and comparing the voltammogram area at each layer deposited.

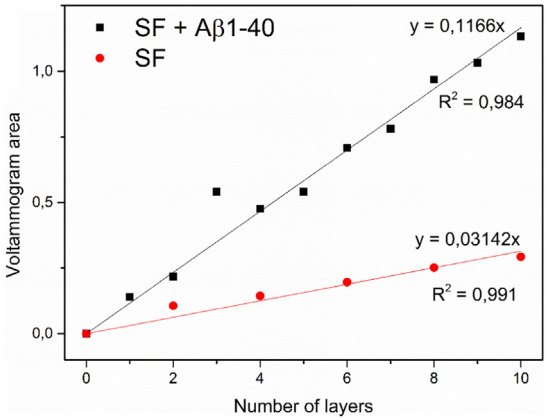

Fig. 3. Voltammogram area as a function of the number of layers adsorbed on screen-printed carbon electrode.

Fig. 3 shows the voltammograms area for each layer deposited of the LbL films containing only SF and SF/Aβ1-40. For the SF film a linear increase in the voltammogram area was observed with the increasing number of layers, i. e. the SF was gradually being adsorbed at the surface of the carbon electrode. For the film containing SF and Aβ1-40 the same characteristics were observed. For each SF and Aβ1-40 layer deposited the voltammogram area increased linearly. Comparing the linear regression of the two film growth, it is noted that the slope of the SF film is almost 4 times lower (0,031) than the SF and peptide (0,117), and from this information it is possible to conclude that the SF/Aβ1-40 film grows better than the SF film, due to the adsorption of both SF and Aβ1-40.

The voltammogram area is related to the charge density on the electrode [25,26], so it is possible to conclude that the more species adsorbed to the electrode, higher the electron density and higher the voltammogram area. In this case, the higher voltammogram areas were obtained in the SF/Aβ1-40 film, confirming that both SF as peptide were adsorbed in the LbL film. The linear increase in the voltammogram area indicating that the film has been deposited uniformly in each layer.

Circular dichroism measurements were carried to analyze the conformation of the peptide in solution and in the film (Fig. 4). The Aβ1-40 peptide spectrum in aqueous solution showed two negative minimum at 226 nm and 209 nm, which are characteristic of an alpha-helix conformation. In fact, nuclear magnetic resonance (NMR) shows a small portion of alpha-helix conformation in aqueous solution [27].

Films of SF using the LbL technique showed a high content of beta-sheet structure [19], as it was observed in Fig. 4, with a minimum at 217 nm. When Aβ1-40 was added to the film, a small shift in that

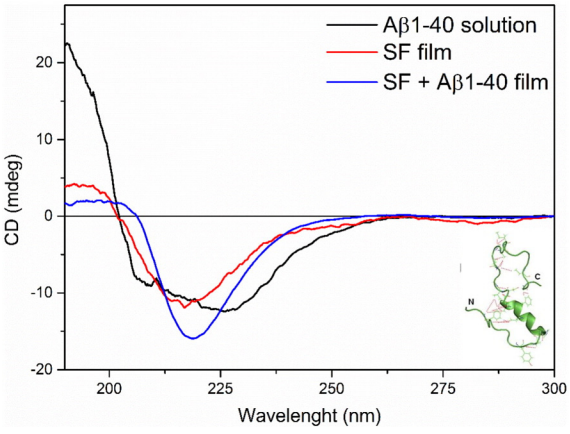

Fig. 4. Circular dichroism spectra of Aβ1-40 in aqueous solution, SF film and SF/Aβ1-40 film. Inset: Aβ1-40 aqueous solution conformation determined by NMR [27].

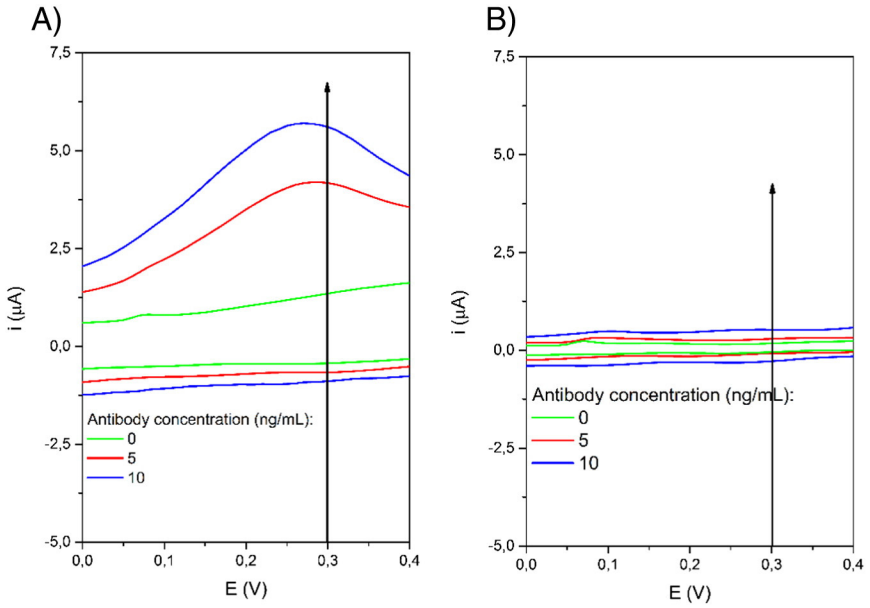

Fig. 5. Cyclic voltammograms of selected antibody concentrations for (A) SF/Aβ1-40 film and (B) SF film.

minimum can be observed (219 nm), indicating that the peptide was successfully adsorbed in the film and probably has its secondary structure preserved. It must be remembered that the secondary structure of the peptide is essential for the antibody-antigen recognition.

After confirming the peptide Aβ1-40 immobilization in conjunction with SF, cyclic voltammetry was performed to test the SF/Aβ1-40 film ability to bind to the specific Aβ1-40 antibody. For this, SF/Aβ1-40 LbL films containing 1, 3 and 5 bilayers were assembled.

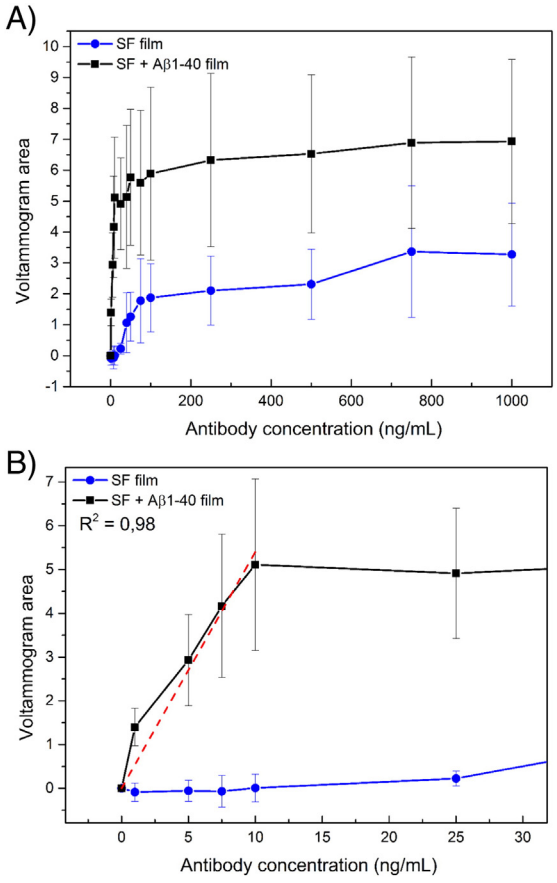

Fig. 6. Electrode response voltammogram area as a function of antibody concentration. (A) Whole area analyzed and (B) Zoom of 0–25 ng mL^{-1} area. $n = 4$.

Fig. 5A and B show the cyclic voltammograms for 1-bilayer SF/Aβ1-40 and 1-layer SF films, respectively, in the presence of different concentrations of antibody. At around 0.3 V, it was possible to observe an increase of the current, i. e., an oxidation peak, for SF/Aβ1-40 film with increasing antibody concentration. This peak was not observed in the SF film (Fig. 4B) indicating the antibody specifically bonded to Aβ1-40, and not to SF. The current difference in the case of SF/Aβ1-40 was 4.26 μA, almost 12 times higher than the difference for the film containing only SF (difference = 0.35 μA). The films containing 3 and 5 bilayers did not show a good response when compared with film containing 1-bilayer, results not showed.

The immunosensor reproducibility was performed using new electrodes and more samples. Three more electrodes with films were prepared and tested, with the same parameters of the experiment above. For the current difference observed previously, the error bars were too high for distinguish the electrode without Aβ1-40 from the electrode containing the peptide, and because of this the data is not shown.

As the results from the current difference were not appropriate for immunosensor applications, the data were analyzed using voltammogram areas. In this case, the immunosensor showed a positive response together with low error bars, as shown in Fig. 6. This result showed that not only the Aβ1-40 antibody specifically recognized its antigen, but the response antigen-antibody was enough to produce a measurable electron density that can identify the presence of antibody in the sample.

The response of the two films (containing or not Aβ1-40) with voltammogram area showed that at the lowest concentration, from 0 to 10 ng mL^{-1} there was an approximately linear response ($R^2 = 0.98$), as showed in Fig. 6B. For higher concentrations, above 10 ng·mL^{-1} to 1000 ng·mL^{-1}, there was a saturation of the bonding sites, *i.e.* all the Aβ1-40 peptides were bonded to an antibody (Fig. 6A). The error bars were calculated for a total of 4 experiments. Note that large error bar can be attributed the insufficient time of antibody adsorption, about 10 min. Time higher than this can increase the adsorption of interfering molecules. However, error bars do not overlap the non-specific response. In the linear range from 0 ng mL^{-1} to 10 ng mL^{-1} the results were reliable, with enough difference between them to be used in further applications.

Although the linear range is short, this method could overcome some disadvantages of other systems described in the literature. With

a very simple and fast electrode modification we were able to successfully detect extremely low concentrations of Aβ1-40, providing another tool for fast measurement of this peptide.

4. Conclusion

A method was presented to immobilize the peptide Aβ1–40 using the LbL technique and SF as opposing electrolyte. The peptide was successfully adsorbed in alternated layers with SF on quartz substrate and also on screen-printed electrodes. The cyclic voltammograms showed an increasing current with the presence of antibodies in the 0.3 V region, and showed a linear response of the voltammogram area *versus* antibody concentration from 0 to 10 ng mL^{-1}.

Acknowledgements

Brazilian agencies CAPES, CNPq and FAPESP are acknowledged.

References

[1] 2014 Alzheimer's disease facts and figures, Alzheimers Dement. 10 (2) (2014) e47–e92, http://dx.doi.org/10.1016/j.jalz.2014.02.001.
[2] R. Brookmeyer, et al., Forecasting the global burden of Alzheimer's disease, Alzheimers Dement. 3 (3) (2007) 186–191, http://dx.doi.org/10.1016/j.jalz.2007.04.381.
[3] A. Wimo, et al., The worlwide economic impact of dementia 2010, Alzheimers Dement. 9 (1) (2013) 1–11, http://dx.doi.org/10.1016/j.jalz.2012.11.006.
[4] M.S. Alberta, et al., The diagnosis of mild cognitive impairment due to Alzheimer's disease: recommendations from the National Institute on Aging-Alzheimer's Association workgroups on diagnostic guidelines for Alzheimer's disease, Alzheimers Dement. 7 (3) (2011) 270–279, http://dx.doi.org/10.1016/j.jalz.2011.03.008.
[5] J.A. Hardy, G.A. Higgins, Alzheimer's disease: the amyloid cascade hypothesis, Science 256 (5054) (1992) 184–185, http://dx.doi.org/10.1126/science.1566067.
[6] W.E. Klunk, et al., Imaging brain amyloid in Alzheimer's disease with Pittsburgh compound-B, Am. Neurol. Assoc. 55 (13) (2004) 306–319, http://dx.doi.org/10.1002/ana.20009.
[7] J.F. Poduslo, et al., Molecular targeting of Alzheimer's amyloid plaques for contrast-enhanced magnetic resonance imaging, Neurobiol. Dis. 11 (2) (2002) 315–329, http://dx.doi.org/10.1006/nbdi.2002.0550.
[8] J.D. Doecke, et al., Blood-based protein biomarkers for diagnosis of Alzheimer disease, JAMA Neurol. 69 (10) (2012) 1318–1325, http://dx.doi.org/10.1001/archneurol.2012.1282.
[9] B.-X. Qu, et al., Beta-amyloid auto-antibodies are reduced in Alzheimer's disease, J. Neuroimmunol. 274 (1–2) (2014), http://dx.doi.org/10.1016/j.jneuroim.2014.06.017 (198-173).
[10] J. Zhou, H. Fa, W. Yin, J. Zhang, C. Hou, D. Huo, D. Zhang, H. Zhang, Synthesis of superparamagnetic iron oxide nanoparticles coated with a DDNP-carboxyl derivative for in vitro magnetic resonance imaging of Alzheimer's disease, Mater. Sci. Eng. C 37 (2014) 348–355, http://dx.doi.org/10.1016/j.msec.2014.01.005.
[11] S. Mirsadeghi, et al., Effect of PEGylated superparamagnetic iron oxide nanoparticles (SPIONs) under magnetic field on amyloid beta fibrillation process, Mater. Sci. Eng. C 59 (2016) 390–397, http://dx.doi.org/10.1016/j.msec.2015.10.026.
[12] E. Kleiren, et al., Development of a quantitative and conformation-sensitive ATR-FTIR biosensor for Alzheimer's disease: the effect of deuteration on the detection of the Aβ peptide, Spectroscopy 24 (1–2) (2010) 61–66, http://dx.doi.org/10.3233/SPE-2010-0405.
[13] S. Prabhulkar, et al., Microbiosensor for Alzheimer's disease diagnostics: detection of amyloid beta biomarkers, J. Neurochem. 122 (2) (2012) 174–381, http://dx.doi.org/10.1111/j.1471-4159.2012.07709.x.
[14] S. Fujii, et al., Electrochemical quantification of the Alzheimer's disease amyloid-β (1–40) using amyloid-β fibrillization promoting peptide, Sens. Bio-Sens. Res. 6 (2015) 7–12, http://dx.doi.org/10.1016/j.sbsr.2015.09.001.
[15] Y. Zhou, et al., Simple colorimetric detection of amyloid β-peptide (1–40) based on aggregation of gold nanoparticles in the presence of copper ions, Small 11 (18) (2015) 2144–2149, http://dx.doi.org/10.1002/smll.201402593.
[16] G. Decher, Fuzzy nanoassemblies: toward layered polymeric multicomposites, Science 277 (5330) (1997) 1232–1237, http://dx.doi.org/10.1126/science.277.5330.1232.
[17] K. Ariga, T. Nakanishi, T. Michinobu, Immobilization of biomaterials to Nano-assembled films (self-assembled monolayers, Langmuir-Blodgett films, and layer-by-layer assemblies) and their related functions, J. Nanosci. Nanotechnol. 6 (8) (2006) 2278–2301, http://dx.doi.org/10.1166/jnn.2006.503.
[18] M. Campàs, C. O'sullivan, Layer-by-layer biomolecular assemblies for enzyme sensors, immunosensing, and nanoarchitectures, Anal. Lett. 36 (12) (2003) 2551–2569, http://dx.doi.org/10.1081/AL-120024632.
[19] C.-Z. Zhou, et al., Silk fibroin: structural implications of a remarkable amino acid sequence, Proteins: Struct. Funct. Bioinf. 44 (2) (2001) 119–122, http://dx.doi.org/10.1002/prot.1078.
[20] G.H. Altman, et al., Silk-based biomaterials, Biomaterials 24 (3) (2003) 401–416 (http://dx.doi.org/1016/S0142-9612(02)00353-8).
[21] C. Vepari, D.L. Kaplan, Silk as a biomaterial, Prog. Polym. Sci. 32 (8–9) (2007) 991–1007, http://dx.doi.org/10.1016/j.progpolymsci.2007.05.013.
[22] X. Wang, et al., Biomaterial coatings by stepwise deposition of silk fibroin, Langmuir 21 (24) (2005) 11335–11341, http://dx.doi.org/10.1021/la051862m.
[23] M.L. Moraes, et al., Immunosensor based on immobilization of antigenic peptide NS5A-1 from HCV and silk fibroin in nanostructured films, Langmuir 29 (11) (2013) 3829–3834, http://dx.doi.org/10.1021/la304404v.
[24] C.W.P. Foo, et al., Role of the pH and charge on silk fibroin assembly on insects and spiders, Appl. Phys. A Mater. Sci. Process. 82 (2) (2006) 223–233, http://dx.doi.org/10.1007/s00339-005-3426-7.
[25] Z. Wang, X. Hu, U. Helmersson, Peroxo sol-gel preparation: photochromic/electrochromic properties of Mo-Ti oxide gels and thin films, J. Mater. Chem. (10) (2000) 2396–2400, http://dx.doi.org/10.1039/B004933F.
[26] H. Yu, et al., Novel MoO_3-TiO_2 composite nanorods films with improved electrochromic performance, Mater. Lett. 169 (2016) 65–68, http://dx.doi.org/10.1016/j.matlet.2016.01.097.
[27] S. Vivekanandan, et al., A partially folded structure of amyloid-beta(1–40) in an aqueous environment, Biochem. Biophys. Res. Commun. 411 (2) (2011) 312–316, http://dx.doi.org/10.1016/j.bbrc.2011.06.133.